Morphology of PDMS−PMAA IPN Membranes

J. S. Turner and Y.-L. Cheng*

Department of Chemical Engineering and Applied Chemistry, University of Toronto, Toronto, Ontario M5S 3E1 Canada

Received December 28, 2001

ABSTRACT: Direct visualization of IPN morphology formed during polymerization-induced phase separation (PIPS) of PDMS−PMAA IPNs is reported. Laser scanning confocal microscopy (LSCM) and hydrophilic fluorescent probes of varying molecular weights were used to image hydrophilic domains in PDMS−PMAA IPNs. The images reveal complex, superimposed structures of hydrophilic domains of varying sizes and spatial distributions. This morphology is attributed to the phase-separated structures formed and partially arrested at continuously varying quench depths during the PIPS process. These observations contribute to the understanding of morphology development in IPNs.

Introduction

IPN morphology is largely determined by phase separation of the polymer components during IPN formation. In sequential IPNs, phase separation occurs as a result of the polymerization and cross-linking of the guest monomers within the host polymer network, a process called polymerization-induced phase separation (PIPS).[1] Increasing the molecular weight of the guest polymer network due to polymerization and cross-linking increases the thermodynamic driving force for phase separation while the accompanying vitrification and increasing viscosity kinetically hinder and may ultimately arrest phase separation. Thus, the morphology formed via PIPS is highly dependent upon the relative rates of the polymerization and cross-linking reactions vs the rate of phase separation.[2]

Quench depth is a quantitative representation of the thermodynamic driving force for phase separation defined as the difference between the actual temperature of an immiscible IPN system and the temperature of incipient miscibility, i.e., either the lower or upper critical solution temperature (LCST or UCST).[3] In PIPS, the phase diagram continually changes as the guest polymer molecular weight increases, resulting in continually varying quench depths. This phenomenon contrasts with the more widely studied thermally induced phase separation (TIPS) in which nonreacting IPN systems or blends are subjected to a stepwise temperature change.[3]

The mechanism by which phase separation occurs and the resulting morphology depend on the region of the phase diagram in which the IPN system is located.[3] In the metastable region, phase separation occurs via nucleation and growth (NG) in which isolated concentration fluctuations with an equilibrium composition initially appear and then grow to yield an irregular two-phase structure.[1] In the unstable or spinodal region of the phase diagram, concentration fluctuations begin small and grow in amplitude and wavelength as phase separation proceeds. Spinodal decomposition (SD) is the predominant mechanism during the formation of IPNs.[4,5]

Extensive studies of SD initiated by TIPS have revealed a four-stage process in morphology formation. During the early stages, a highly interconnected, two-phase morphology with a unique periodicity or a domain structure with relatively narrow size distributions may be obtained. As phase separation progresses, both the concentration and size of the separated domains increase and the interconnected structure yields fragmented domains followed by spherical domains that may grow in size and coalesce. The domain sizes during TIPS, even in the late stages of SD are of a uniform size and dispersed quite regularly.[1]

Although similar stages of SD were found to occur in PIPS, there has been some indication in the literature[6,7] that PIPS-induced SD in IPNs does not produce uniform domain sizes. This has been attributed to the time-variant nature of quench depth in this process. It has been reported that the size of phase separated domains is inversely proportional to quench depth;[8,9] thus, the continuous change in quench depth during PIPS should result in a variety of domain sizes in the final IPN morphology.[6,7] However, either a single domain size or evidence of only two different domain sizes has been reported.[10,11]

Chou et al.[10] examined morphology development in a polyurethane (PU) and polystyrene (PS) IPN using phase-contrast optical microscopy and transmission electron microscopy (TEM). An interconnected phase developed, which coalesced to form a periodic droplet and matrix type morphology. A second level of phase separation producing smaller domains was found to occur within the droplet and matrix phases produced by SD. Widmaier[11] examined semi-IPNs of cross-linked PU and linear PS by light transmission studies, optical microscopy, and scanning electron microscopy (SEM) and found that when the reaction medium phase separated before gelation of PU, the final morphology was a superposition of two levels of phase separation: (i) a fine dispersion of the components and (ii) a gross phase separation of PS noduli surrounded by a PU-rich shell. Although these limited examples allude to a more complex morphology formed in IPNs due to PIPS, they only directly demonstrate the existence of two phase separated domain structures with widely different length scales.

In a previous paper,[12] it was shown that PDMS−PMAA IPNs prepared using a monomer immersion method formed a bicontinuous morphology consisting

* Corresponding author. Telephone: 1-416-978-5500. Fax: 1-416-978-8605. E-mail: ylc@chem-eng.utoronto.ca.

10.1021/ma012253y CCC: $25.00
Published on Web 02/28/2003

of hydrophilic PMAA channels within a PDMS matrix. When these IPNs were immersed in solutions of hydrophilic fluorescent probes, the probes were distributed through the interconnected PMAA hydrogel domains, but were excluded from PDMS regions and inaccessible PMAA domains. Observations using laser scanning confocal microscopy (LSCM) showed that interconnected hydrogel domains that contained the fluorescent probe were visible and distinguishable from the rest of the IPN. In this paper, the morphology of PDMS−PMAA IPNs is further examined by using fluorescent markers of different molecular weights to probe the size distribution of PMAA hydrogel domains within the IPNs.

Experimental Section

Preparation of PDMS−PMAA IPNs. PDMS−PMAA IPN membranes were prepared using the monomer immersion method described in detail in an earlier paper.[12]

Briefly, PDMS films were first prepared by mixing vinyl-terminated poly(dimethylsiloxane) resin (116 000 Da, 65 000 cst) with 10% hydride terminated PDMS (1000 cst) and 60 ppm of platinum divinyltetramethyldisiloxane complex (all from United Chemical Technologies, Bristol, PA) and 4% of a cyclic, multifunctional silicone hydride cross-linker MDX4−4210 (Dow Corning, Midland, MI). The mixture was then spread to 0.5 μm thickness on a Mylar sheet, and degassed under a vacuum of 25 mmHg for 6 h. Hydrosilyation addition and cross-linking were then carried out at 55 °C for 24 h. Cross-linked PDMS was then washed in cyclohexane for 24 h.

IPN membranes were then prepared by immersing a film of cross-linked PDMS in a methacrylic acid (MAA) monomer solution containing 1% w/v of 2,2-dimethoxyacetophenone and 1% v/v of triethylene glycol dimethacrylate (TEGDMA) cross-linker for approximately 18 h at room temperature. The monomer swollen PDMS network (pre-IPN film) was then immersed in a MAA monomer solution that contains no cross-linking agent or photoinitiator and irradiated with 32 W intensity, 350 nm UV light for 1 h to produce the IPN. Cross-linking agent and photoinitiator were excluded from the immersion medium to prevent the solidfication of the medium and IPN entrapment. The IPN contained approximately 30% PMAA on a dry basis.

LSCM of IPN Morphology. The morphology of the PDMS−PMAA IPN prepared according to the monomer immersion method was examined as a function of depth via LSCM (Carl Zeiss LSCM 510) using the procedure described in a previous paper.[12] Pieces of PDMS−PMAA IPN membranes were placed in solutions of different molecular weight fluorescent probes for 1 month: a 200 ppm solution of fluorescein (sodium salt, MW 332 Da), and 3000 ppm solutions of fluorescein isothiocyanate dextran of 4400 Da (FDX4.4KD) and 70 000 Da (FDX70KD) molecular weights. These hydrophilic markers permeated the interconnected hydrogel domains of the IPN and were used to distinguish the accessible hydrogel domains from the PDMS regions and inaccessible hydrogel domains of the IPN. Each IPN section was imaged at depths of 2 μm intervals from the IPN surface to approximately 100 μm below the surface. At beyond 100 μm depths, the images were too dark and unfocused to be useful.

Immersion in dye solutions for longer than 1 month gave the same confocal microscopy images—suggesting that equilibration had been reached at 1 month or that diffusion into some regions of the IPNs was so slow that no dye transport was visible even at 1 month. Experiments showed that different lateral sections of the same pieceof IPN gave the same confocal images when probed with the same dye at the same depth—indicating that there is no lateral variation in morphology. The images obtained with different molecular weight probes reported in the manuscript are also from different sections of the same piece of IPN; these different sections should have the same morphology, and therefore, the images should be superimposable.

Results

LSCM images of PDMS−PMAA IPNs that had been preequilibrated with solutions of FDX4.4KD, or FDX70KD are shown in Figures 1 and 2, respectively. The red regions represent PMAA hydrogel domains that were accessible to the probe, while the black regions represent parts of the IPN from which the probe was excluded. Probes may be excluded from PDMS regions, as well as PMAA regions that have a domain size or mesh size that are smaller than the probe molecule. Since it is believed that phase separation occurs via spinodal decomposition,[12] it is unlikely that there are PMAA regions that are inaccessible because they are isolated in a sea of PDMS.

The LSCM images of an IPN that had been preequilibrated with a fluorescein solution are not shown here because they are identical in appearance to Figure 1, parts a and b, the surface and 50 μm depth images of FDX4.4KD equilibrated IPN's. At selected depths up to 150 μm, fluorescein-equilibrated IPN's showed small red cylindrical regions homogeneously dispersed throughout a continuous black region. A comparison of fluorescein hydrodynamic diameter (0.8 nm) and the size of a repeat unit in PMAA indicates that it is unlikely for fluorescein to be excluded due to a smaller mesh size in the hydrogel regions. The black region should therefore represent PDMS. In these images, the PMAA gel domains appear to be uniformly dispersed and of the same approximate size.

Figure 1 shows LSCM images of PDMS−PMAA IPN preequilibrated in a concentrated solution of FDX 4.4KD (h.d. 9.4 nm). Images of the first 50 μm of the membrane were similar to images of the fluorescein-equilibrated IPN. The domains appeared small, of uniform size and homogeneously dispersed. Beyond 50 μm, LSCM images of the IPN cross-section abruptly changed. Large black regions, indicating an absence of fluorescent solute, and red regions that formed a macrostructure containing smaller, red cylindrical gel domains, were observed. In Figure 1c at a depth of 52 μm, a macrostructure of gel domains is visible which is similar to that of intermediate-stage spinodal decomposition, where the interconnected cylindrical domains had grown in size and become globular in order to minimize the interfacial area. At 54 μm, the macrostructure appears as spherical domains (Figure 1d) similar to late stage SD. Parts e and f of Figure 1 show a connected globular structure. It was also evident that the larger spherical domains contained smaller cylindrical gel domains.

Parts a−f of Figure 2 contain LSCM images of the PDMS−PMAA IPN preequilibrated with a solution of FDX70KD (h.d. = 37.4 nm). In contrast to the smaller probes, the nonrandom distribution of accessible domains was evident at just 5 μm from the surface (Figure 2b), where clusters of red regions and black regions had formed. At a depth of 10 μm (Figure 2c), a large decrease in the volume fraction of gel domains accessible to FDX70KD is seen. The upper left-hand corner contained an area of very small, spherical, gel regions similar to morphology created by the NG mechanism of phase separation. At 15 μm (Figure 2d), larger globules of a similar diameter containing smaller cylindrical gel domains were evident. Globules of even larger sizes, some of which appear to have coalesced, are visible at 20 (Figure 2e) and 25 μm (Figure 2f). This morphology is similar to that created in the late stages of the SD mechanism.

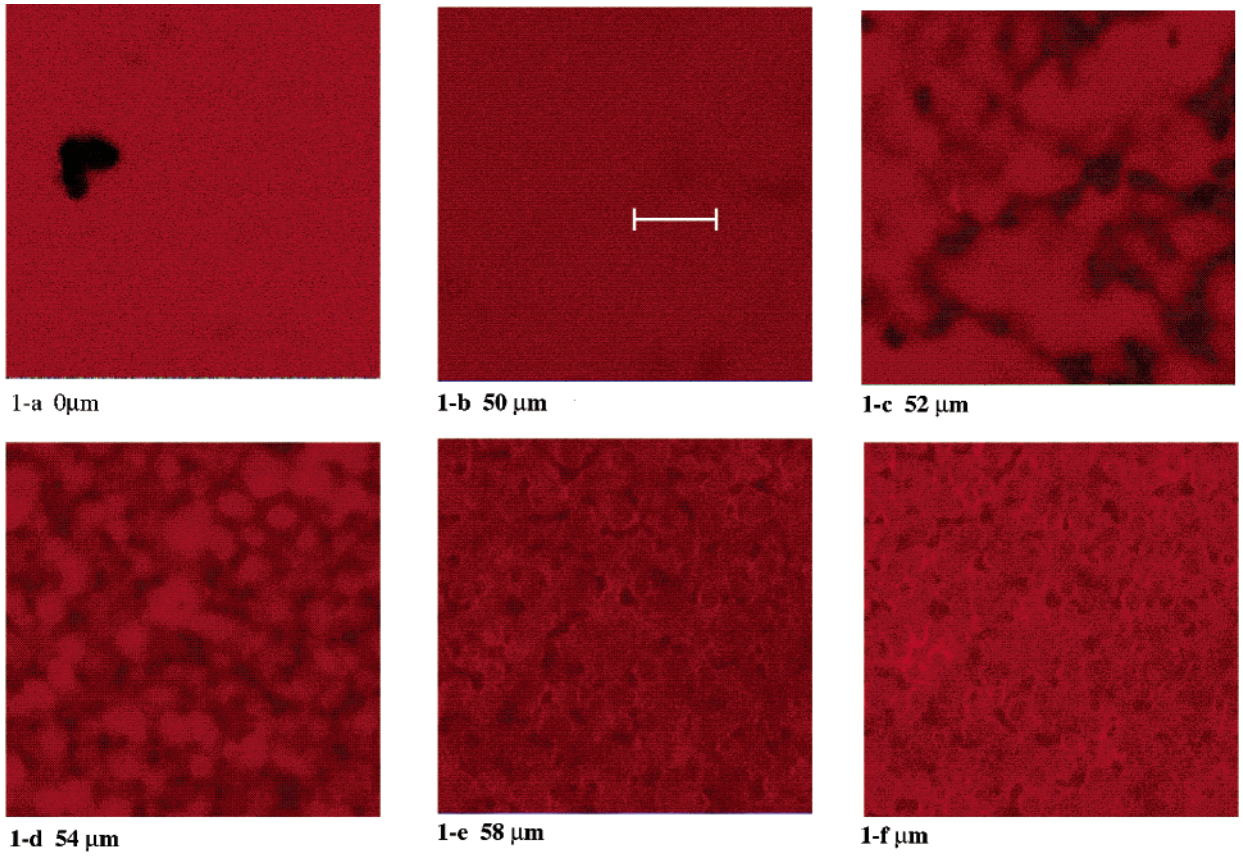

Figure 1. LSCM images of PDMS−PMAA IPN immersed in FITC−dextran (4400 Da) solution as a function of depth (scale bar = 5 μm).

Discussion

PDMS−PMAA IPN Morphology Imaged Using Different Size Probes. The literature on PIPS-induced IPN morphology includes experimental evidence of uniform domain size morphology and a theoretical understanding that supports a continuum of domain sizes with a few experimental examples of IPNs having multiple length scales. TEM[13,14] or SEM[15,16] studies have produced IPN images with uniform size and distribution of gel domains, and suggested that PIPS results in IPN morphology similar to the morphology of polymer blends produced by TIPS. These conclusions have been questioned[2,6] because PIPS and TIPS are fundamentally different processes. In particular, since it is known that phase separation is determined by quench depth and quench depth increases continuously during PIPS, the continually varying quench depth during PIPS should result in a distribution of gel domain sizes in the final IPN morphology. The results of the current study provides visual evidence to support the presence of a distribution of gel domain sizes.

LSCM images of fluorescein-equilibrated IPN's show that gel domains in the first 150 μm of the IPN that are accessible to the 0.8 nm fluorescein probe are homogeneously dispersed and uniform in size. A comparison of Figure 1 shows that at 50 μm depth and below, some of the fluorescein-accessible domains are inaccessible to the 9.4 nm FITC-dextran probe. Further comparison with Figure 2 shows that at just 5 μm below the surface, a fraction of the fluorescein-accessible domains are inaccessible to the 37.4 nm FITC-dextran probe. These observations indicate that gel domains of at least three different ranges of length scales, representing different accessibility to the three probes, coexist within the IPN at varying depths. The discrete nature of the probe dimensions does not allow finer resolution of domain sizes, but these observations strongly suggest that a continuum of domain length scales may exist.

It is proposed that the different gel domain length scales are a result of the morphology created at different quench depths during polymerization and cross-linking of the IPN. At shallow quench depths in the early stages of PIPS, i.e., shortly after the point of incipient phase separation, when the system conditions coincide with the boundary between miscible and immiscible regions of the phase diagram, phase separation may occur by either NG or SD. NG is known to produce relatively large and well-separated domains[4] that are spherical in shape and nonuniform in size. With the largest probe used, evidence for such domains can be seen in Figure 2c. SD at shallow depths are also known to produce relatively large domains [1], but SD-produced domains are known to have approximately the same size and spacing and are usually connected or have coalesced with growth. Evidence for large domains of SD type morphology is seen in Figure 2, parts d−f. As polymerization and cross-linking reactions progress, it is expected that SD will become the dominant mechanism of phase separation and the gel domains formed at deeper quenches will be much smaller.[1] These smaller gel domains may form within the larger domains formed earlier, so that depending upon the size of the permeating probe, images may show smaller domains contained within larger ones (Figures 1c and 2d−f), or they may show evidence of only the smaller domains.

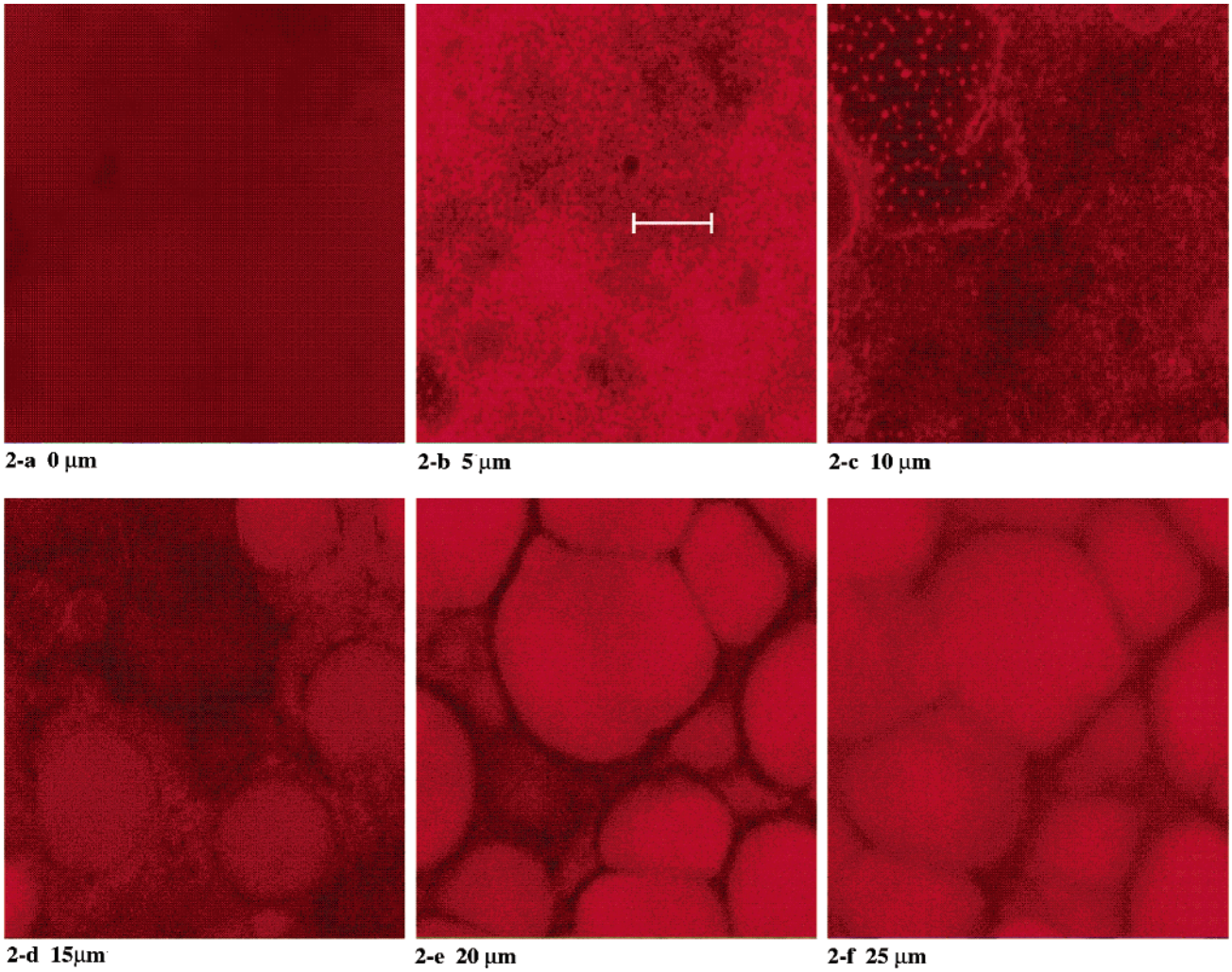

Figure 2. LSCM images of PDMS−PMAA IPN immersed in FITC−dextran (70 000 Da) solution as a function of depth (scale bar = 5 μm).

The literature contains only a few examples of IPNs having different length scales. Tran-Cong et al.[2] indirectly demonstrated the existence of domains of two different length scales during photocrosslinking of two components of a ternary polymer blend. Using a phase-contrast optical microscope and a two-dimensional fast Fourier transform image analysis method, they were able to distinguish between the different sized domains formed in the cross-linked polymer blend. This morphology was attributed to the inhomogeneous freezing kinetics of the cross-linking process.

Yang et al.[17] prepared semi-IPNs from polyphenyl ether and cross-linked poly(diallyl phthalate). They observed systems of fine polyDAP domains on the order of 10 nm present in the larger, micrometer-size dispersed particles using TEM. They concluded that the fine domains were formed by successive SD, under very deep quench after the micrometer scale particle/matrix morphology had been arrested by partial cure. This morphology was similar to that observed in Figure 2, parts d−f.

Harada[18] observed NG type structures similar to those in Figure 2c using phase-contrast optical microscopy at different time intervals for a polymer blend cross-linked by irradiation. The appearance of nuclei was first noted, followed by the appearance of interconnecting structures around the nuclei at later times. This process was termed nucleation-assisted SD.

Only isolated examples of different domain sizes have been provided in the literature, perhaps because the analytical methods used to examine IPN morphology were not able to distinguish between the various levels of phase separation and domain structures present. The analytical techniques that have been used to investigate IPN morphology include TEM, SEM, phase-contrast optical microscopy, and, to a lesser extent, small-angle neutron scattering and SAXS.[21] For each of these methods all the domains present are imaged at one time so that images are similar to those in Figure 1. Not surprisingly, studies using these methods have concluded that IPNs consist of a single domain length scale. The probe method used in this study provides a means of distinguishing complex, multilayered morphology with multiple length scales in IPNs.

PDMS−PMAA IPN Gel Domain Morphology as a Function of Depth. Figures 1 and 2 can be compared to see how IPN morphology and domain size varied as a function of depth. The morphology of fluorescein accessible regions was uniform throughout the first 150 μm of the IPN surface region while gel domains of larger length scales varied with depth). In Figure 1c at 52 μm, a macrostructure of gel domains formed which was similar to that of intermediate-stage SD. A similar pattern of morphology as a function of depth is seen in Figure 2, parts d−f.

This variation in morphology with depth was attributed to the different kinetics of polymerization and cross-linking that occurred as a function of depth due to the nonuniform distributions of cross-linker, initiator, and UV intensity. UV intensity was expected to decrease with depth due to interference from the polymer. Cross-linker and initiator concentrations decreased toward the surface of the IPN due to diffusion out into the surrounding monomer during IPN formation. The LSCM observations are consistent with more rapid polymerization kinetics near the surface than in the interior of the IPN.

If polymerization progresses much faster than phase separation, then phase separation occurs primarily at deep quench, and smaller domains would be expected as is seen near the surface. With slower polymerization kinetics, quench depth would change more slowly and phase separation occurring at shallow quench depths would be significant producing larger domains. At 50 μm depths from the surface (Figure 1c) there was evidence of late stage SD where SD at shallow quench was allowed to proceed to near completion. This was attributed to phase separation that was faster than polymerization and cross-linking due to the decrease in UV light intensity at this depth.

Conclusions

Direct visual evidence of a complex array of morphological structures in IPNs formed via PIPS has been presented. Images were obtained by preequilibrating IPNs with different size fluorescent probes, and visualizing the fluorescent regions using LSCM. The evidence is consistent with a complex series of phase separations produced at different quench depths during PIPS and arrested by partial cure to form the final structure of the IPN. A variety of domain sizes and macrostructures coexisted at any given depth in the IPN. Morphology also varied with depth due to gradients in initiator concentration, cross-linking agent concentration and UV light intensity during IPN formation. This work contributes to an improved understanding of morphology development that takes place during the PIPS process of IPNs.

References and Notes

(1) Inoue, T. *J. Controlled Release* **1995**, *39*, 109.
(2) Tran-Cong, Q.; Kawai, J.; Nishikawa, Y.; Jinnai, H. *Phys. Rev. E* **1999**, *60*, R1150-r1153.
(3) Kiefer, J.; Hedrick, J. L.; Hilborn, J. G. *Adv. Polym. Sci.* **1999**, *147*, 161−247.
(4) Sperling, L. H. Interpenetrating Polymer Networks: An Overview. In *Interpenetrating Polymer Networks*; Klempner, D., Sperling, L. H., Utracki, L. A., Eds.; Advances in Chemistry Series 239; American Chemical Society: Washington DC, 1994; pp 1−43.
(5) Lipatov, Y. S.; Nesterov, A. E. Mechanism and Kinetics of Phase Separation in Polymer Solutions and Blends. In *Thermodynamics of Polymer Blends*; Lipatov, Y. S., Nesterov, A. E., Eds.; Technomic Publishing: Lancaster, PA, 1997; pp 275−362.
(6) Tran-Cong, Q.; Kawai, J.; Endoh, K. *Chaos* **1999**, *9*, 298−307.
(7) Seul, M.; Andelman, D. *Science* **1995**, *267*, 476−483.
(8) van Aarsten, J. J. *Eur. Polym. J.* **1970**, *6*, 919.
(9) Binder, K.; Stauffer, D. *Phys. Rev. Lett.* **1973**, *33*, 1006.
(10) Chou, Y. C.; Lee, L. J. *Polym. Eng. Sci.* **1994**, *34*, 1239−1249.
(11) Widmaier, J. M. *Macromol. Symp.* **1995**, *93*, 179−186.
(12) Turner, J. S.; Cheng, Y. Preparation of PDMS−PMAA IPNs Using the Monomer-Immersion Methodology. *Macromolecules* **2000**, *33*, 3714−3718.
(13) Burford, R.; Chaplin, R.; Mai, Y. M. In *Multiphase Macromolecular Systems*; Culbertson, M., Ed.; Plenum: New York, 1989;.
(14) Donatelli, A. A.; Sperling, L. H.; Thomas, D. A. *Macromolecules* **1976**, *9*, 671−676.
(15) Chen, X.; McGurk, S. L.; Davies, M. C.; Roberts, C. J.; Shakesheff, K. M.; Tendler, S. J. B.; Williams, P. M. *Macromolecules* **1998**, *31*, 2278−2283.
(16) Yeo, J. K.; Sperling, L. H.; Thomas, D. A. *Polymer* **1983**, *24*, 307.
(17) Yang, Y.; Fujiwara, H.; Chiba, T.; Inoue, T. *Polymer* **1998**, *39*, 2745−2750.
(18) Harada, A.; Tran-Cong, Q. *Macromolecules* **1997**, *6*, 11643−1650.
(19) Tran-Cong, Q.; Okinaka, J. *Polym. Eng. Sci.* **1999**, *39*, 365−370.
(20) Kim, Y.; Kim, S. *Macromolecules* **1999**, *32*, 2334−2341.
(21) Hourston, D. J.; Song, M.; Schafer, F. U.; Pollock, H. M.; Hammiche, A. *Thermochim. Acta* **1998**, *324*, 109−121.

MA012253Y